Electronic Supplementary Material (ESI) for Chemical Science.
This journal is © The Royal Society of Chemistry 2022

Electronic Supporting Information

Construing the metaxin-2 mediated simultaneous localization between mitochondria and nucleolus using molecular viscometry

Table of Contents

1. Materials and Instrumentation……3

2. Geometry Optimization of **QR**……3

3. Molecular docking and Molecular dynamics (MD) simulation ……3-4

4. Experimental Section……4

4.1. Steady-state absorption and fluorescence experiments……4

4.2. Determination of partition coefficient……4-5

4.3. Cell culture and imaging……5

4.4. Culture method……5

4.5. Cytotoxicity assay……5

4.6. Mitochondrial potential uncoupling assay by CCCP……5

4.7. Induced apoptosis assay by Etoposide……5

4.8. Monensin treatment……6

4.9. Confocal microscopy……6

4.10. Flow cytometry……6

5. Equations used……6-7

6. Figures & Table……7 – 19

Fig. S1: HOMO and LUMO pictures of **QR**……8

Table S1: Photophysical data of **QR** in different solvents and media……8

Fig. S2: Plot of photostability, lifetime, and log τ vs. log η of **QR**……9

Fig. S3: pH titration (absorption) of **QR**……9

Fig. S4: pH titration (emission) of **QR**……10

Fig. S5: Temporal viscosity sensitivity of **QR**……10

Fig. S6: Cell viability plot of **QR**……..11

Fig. S7: CLSM images of live-cell colocalization studies of **QR** with ER and LysoTracker green……..11

Fig. S8: CLSM images of **QR** stained CHO cells……..12

Fig. S9: CLSM images (with ROI) of monensin-treated live cells……..12

Fig. S10: CLSM images (with ROI) of CCCP and Etoposide treated live cells……..13

Fig. S11: Flow cytometry analysis……..13

Fig. S12: JC-1 assay by fluorescence microscopy……14

Fig. S13: DCFDA (2',7'–dichlorofluorescin diacetate) assay for ROS detection……15

Fig. S14. MTX2-**QR** interaction monitored throughout MD simulation ……..16

Fig. S15. The root mean square deviation (RMSD) in displacement of MTX2-QR……16-17

Fig. S16. The root mean square fluctuation (RMSF) of MTX2-QR……..17

Fig. S17. CLSM images of RNA digestion experiment……..18

Fig. S18: CLSM images showing mitochondrial morphology……19

References……..19

1. Materials and Instrumentation

Quinaldine Red (**QR**) and 2',7'–dichlorofluorescin diacetate (DCFDA) were purchased from Sigma Aldrich (USA) and used without any purification. All spectroscopic solvents were procured from Sisco research laboratories Pvt. Ltd. (SRL). Sodium phosphate (monobasic and dibasic) was purchased from Central Drug House Pvt. Ltd.; sucrose purchased from Otto Chemie Pvt. Ltd. was used as received. Milli-Q water was used for the preparation of the buffer used in spectroscopic measurements. For all experiments, a 1 mM stock solution of the dye was prepared in spectroscopic grade DMSO and was diluted appropriately. Sucrose solutions (% w/w) were prepared in 10 mM PBS, pH 7.4. The organelle staining agents Hoechst 33342, MitoTracker green, ER-Tracker green, and LysoTracker green were procured from Thermo Fisher Scientific (USA). The ionophore monensin, protonophore carbonyl cyanide *m*-chlorophenylhydrazone (CCCP), etoposide, and doxycycline hydrochloride were purchased from Sigma Aldrich (USA). Ciliobrevin D and JC-1 dye were purchased from MedChemExpress (USA).

The absorption and emission spectra were recorded on a UV-Vis. spectrophotometer (Shimadzu UV-1800) and fluorimeter (Fluorolog 3, HORIBA Jobin Yvon) respectively, using a 10 mm path length quartz cuvette. Temperature-dependent PL spectra were recorded with a temperature controller (TC1, Quantum northwest) attached with the Fluorolog. Time-resolved fluorescence measurements were performed using a time-correlated single-photon counting (TCSPC) unit (Hamamatsu). The pulse diode laser used was 510 nm with a setup target of 10,000 counts.

2. Geometry Optimization of QR

The geometry optimization and HOMO-LUMO energy gap calculation of **QR** were performed employing density functional theory (DFT) based molecular module DMol3 in the Material Studio 2017 program package.[1] Perdew-Burke-Ernzerhof correlation functional (PBE) was used for all the geometry optimization.[2]

3. Molecular Docking and MD simulation

For the visualization and blind docking, Chimera v1.16 and QVina2.1 were used. The system was prepared using the protein preparation wizard and the minimized structure was exported from the maestro. In Chimera using the structure and binding option under the tools menu, AutoDock Vina was chosen. Output files were named accordingly. Receptors and ligands were chosen. Grid boxes were generated for each protein just to cover the whole protein structure. Hydrogens were added and non-polar hydrogens were removed; non-standard side chains and residues were ignored. In the ligand option, charges were merged and lone pairs were removed. The highest -ΔG values from the scoring matrix were selected to prepare for the Molecular Dynamics simulation.

Protein preparation wizard in Maestro 2020.1, where bind orders were restructured using CCD database base, hydrogens were added, and disulfide bonds were created. The pH of the heteroatoms was maintained to 7.0+- 2.0 using Epik in protein preparation wizard. The docked structure was optimized for sampling water orientations and generation of protein state at pH 7.0. Restrained energy minimization

was done using the OPLS2005 force field. The system was built using Desmond system builder. The model was solvated using the TIP3P water model. Box volume was measured using minimize the volume and the OPLS2005 force field was used for the water model. Ions were used to neutralize the charge of every docked structure placing them 30 Å away from the ligand using the excluded ion placement option. The concentration of salt was 0.15 M NaCl. Molecular Dynamics simulation was performed using the Desmond module with the prepared system set to simulate for 100 ns with recording at every 20 ps producing a total of 5000 frames. The system was relaxed using the default Desmond script. Upon simulation, molecular trajectories, Root Mean Square Deviation (RMSD) of protein-ligand complex, and residues making contacts were analyzed using the Desmond Simulation event analysis tool using default parameters.[3, 4]

4. Experimental Section

4.1. Steady-state absorption and fluorescence experiments:

Ethylene glycol and phosphate buffer mixed at an appropriate ratio were used directly for spectroscopic measurements. Viscosity-dependent spectroscopic experiments were performed with sucrose solutions (5-70% w/w). For this, appropriately weighed sucrose was dissolved in PBS, pH 7.4 to prepare solutions of various viscosities; the solutions were heated in a water bath kept at 318 K if required before use to dissolve any solid precipitated. 10 μL of the stock solution (1 mM) of **QR** was mixed in 1 mL of sucrose solutions of various concentrations, the solutions, kept in tightly sealed vials, were incubated overnight in a shaker maintained at 310 K to achieve homogenous mixing of the components. All solutions were carefully transferred to quartz cuvettes to avoid volume errors. The absorption spectra were recorded at 0.2 nm intervals keeping scan speed medium, and PL measurements were performed keeping $\lambda_{ex/em}$ = 480/500 nm at slit width 1 nm each. All measurements were performed at room temperature (295 K) unless mentioned otherwise.

10 μM solution of **QR** in different % (w/w) aqueous solution of sucrose was used for time-resolved fluorescence measurements. The instrument response function was measured before fluorescence lifetime measurements using a colloidal silica solution (Ludox). All of the decay curves were fitted using the supplied DAS v6.2 software. All measurements were done at room temperature (298 K). A magic angle (54.7°) configuration was used for all measurements. All fittings were done by keeping the χ^2 value within the range of 0.9-1.2.

4.2. Determination of partition coefficient: [5]

A 10 μM solution of **QR** was prepared in n-octyl alcohol and water. The pH of the aqueous phase was adjusted to 7.4 before the experiment. An appropriate aliquot was mixed to make a 1:1 final solution and was shaken for 24 h at 298 K in the dark in a shaker incubator. The next day the mixture was allowed to stand for an adequate time. An aliquot from each phase was withdrawn and the absorbance was measured. The concentration of the dye in each phase was calculated by putting the OD value in a

calibration curve of the dye in that particular phase. The experiment was carried out in triplicates to report the standard deviations present.

4.3. Cell culture and imaging:

Materials: Dulbecco's Modified Eagle Medium (DMEM), Fetal Bovine Serum (FBS), and L-Glutamine-Penicillin-Streptomycin solution (antibiotic cocktail) were purchased from HiMedia (USA). The cell imaging dishes were obtained from Ibidi (Germany).

4.4. Culture method:

U-87MG glioblastoma cell lines were obtained from National Center for Cell Science, and cultured in DMEM (phenol red free) containing 10% (v/v) FBS and 1% (v/v) antibiotic cocktail in 5% CO_2 at 310 K (37 °C) in the incubator. For imaging purposes, cells were grown to 75 – 80% confluency in the 35 mm glass-bottom imaging dishes (170 ± 5 μm).

4.5. Cytotoxicity assay:

Around 5,000 cells per well were seeded in a 96 well-plate and grown for 24 h in 5% CO_2 at 310 K (37 °C) in the incubator. After that, **QR** was added from a 1 mM DMSO stock. The added amount of DMSO was not more than 2 μL. After 24 h of incubation, 20 μL of MTT (3-(4,5-Dimethylthiazol-2-yl)-2,5-Diphenyltetrazolium Bromide) dye solution (from a stock of 5 mg/ mL in PBS 7.4 buffer) was added to each well and incubated for 4 h. The media was removed gently from each well and 100 μL DMSO was added to each well to dissolve the purple-colored crystal. The absorption at 570 nm was recorded in a Synergy H1 Hybrid Multi-mode microplate reader from Biotek.

4.6. Mitochondrial potential uncoupling assay by CCCP:

Live U-87 MG cells were grown in 35 mm glass bottom imaging dishes for 24 h at a density of 2 x 10^5.mL^{-1}. The cells were treated with 5 μM **QR** for 15 minutes and washed twice with PBS 7.4. The cells were imaged under a confocal microscope and a particular field of view was fixed for further comparison. Thereafter, the CCCP solution was carefully added to the imaging dish without disturbing the fixed field of view. The sample was imaged at different desired time points and image analysis was performed.

4.7. Induced apoptosis assay by Etoposide:

Live U-87 MG cells were grown in 35 mm glass bottom imaging dishes for 24 h at a density of 2 x 10^5.mL^{-1}. Firstly, the cells were stained with 5 μM **QR** for 15 minutes followed by the washing step. The stained cells were imaged under a confocal microscope and a particular field of view was fixed for further comparison. Thereafter, the working Etoposide solution was carefully added to the imaging dish without disturbing the fixed field of view. The sample was imaged at different desired time points.

4.8. Monensin treatment:

Live U-87 MG cells were grown in 35 mm glass bottom imaging dishes for 24 h at a density of 2 x 10^5.mL^{-1}. Following the same staining (with **QR**) and washing procedure, cells were exposed to monensin solution and imaged under a confocal microscope. The image analysis was performed using ImageJ v1.53q.

4.9. Confocal microscopy:

All the confocal microscopy imaging was performed with an Olympus FV3000 Confocal Laser Scanning Microscope (CLSM) with live-cell imaging set up. The image processing was done with the help of cellSens Dimension software (Olympus). For fluorescence imaging, 488 nm (MitoTracker green, ER-Tracker green, and LysoTracker green) and 561 nm (**QR**) excitation lasers were used. For 488 nm and 561 nm excitation, the emission windows were kept at 500-540 nm, and 570-670 nm respectively. The confocal aperture was kept at 1.0 Airy Disk (AU) while the dwell time is 8 μs/pixel. The laser power, gain and offset were kept the same for all image acquisitions. The colocalization microscopic experiments have been performed with 5 μM **QR** and 0.3 μM commercial tracker dye incubating for 15 minutes at 310 K (37 °C) in the CO_2 incubator. The images were acquired in sequential scan mode which ensures that the two fluorophores are not excited simultaneously.

4.10. Flow cytometry:

Live U-87 MG cells were seeded at a density of 3 x 10^5 in T-25 culture flasks and cultured overnight at 37 °C in a 5% CO_2. Cells were washed and incubated with monensin for 4 h. Thereafter, the cells were washed with PBS and detached using 1X trypsin-EDTA solution. The post-centrifuged cell pellets were washed twice with cold PBS. Then the cells pellets were gently mixed in a staining solution of **QR** (10 μM **QR** in 1 mL 1X PBS 7.4) and incubated for 15 minutes. The samples were analyzed using BD FACS Aria-II flow cytometer (Becton Dickinson & Company, USA) and data analysis were performed using FlowJo v10.8.1 software (Becton Dickinson & Company, USA).

5. Equations used:

To correlate the fluorescence response and lifetime of **QR** with the viscosity of the medium the Förster-Hoffmann equation was followed.[6]

$$\log I = x \log \eta + C \qquad \textbf{Eqn. S1}$$

and

$$\log \tau = C + x \log \eta \qquad \textbf{Eqn. S2}$$

'I' represent the intensity at emission maxima, τ is the fluorescence lifetime, η is the viscosity of the medium, *C* is constant, and x is the sensitivity of the dye **QR**.

The fluorescent quantum yield of **QR** in various solvents was ascertained with Fluorescein as standard. The following equation was used for the calculation of quantum yields.[7]

$$\Phi_{QR} = \Phi_{\mathrm{Ref}} \times \frac{\eta^2}{\eta_{\mathrm{Ref}}^2} \times \frac{\mathrm{I}}{\mathrm{I}_{\mathrm{Ref}}} \times \frac{\mathrm{A}_{\mathrm{Ref}}}{\mathrm{A}} \qquad \textbf{Eqn. S3}$$

Φ stands for quantum yield. A, I, and η represent the optical density at λ_{ex}, the corresponding relative integrated fluorescence intensity, and the refractive index for each solvent, respectively. The subscript 'Ref' signifies the standard.

6. Figures and Table:

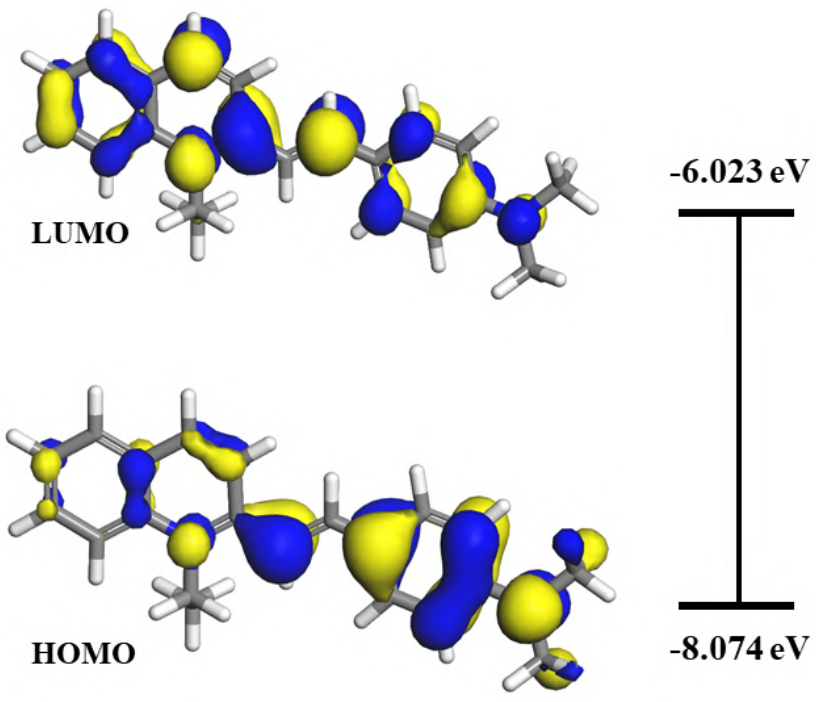

Fig. S1. HOMO and LUMO picture of **QR** obtained from DMol3 in the Material Studio 2017 program package using Perdew-Burke-Ernzerhof correlation functional.

Table S1. Photophysical data of **QR** in different solvents and media

Solvents	ACN	MeOH	DMF	EtOH	DMSO	EG	SUC	GLY
η**/ cp**	0.37	0.60	0.796	1.20	2.24	16.1	480.6	1412
QY	0.003	0.007	0.007	0.016	0.001	0.031	0.072	0.21
$\lambda_{max(em)}$**/ nm**	654	637	651	628	645	642	634	633
E_T**(30)**	45.6	55.4	43.2	51.9	45.1	56.3	--	--
$\lambda_{max(abs)}$**/ nm**	519	525	526	530	528	532	528	536

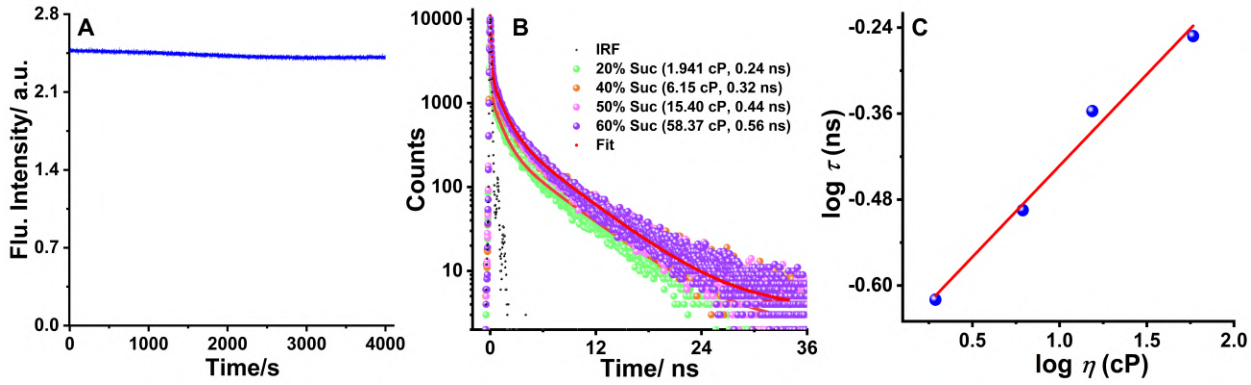

Fig. S2. (A) Plot of fluorescence intensity of 10 μM **QR** in 70% aqueous solution of sucrose at 640 nm vs. time (sec) using steady-state fluorescence experiment, **(B)** time-resolved fluorescence decay curve of 10 μM **QR** in 20%, 40%, 50%, and 60% aqueous solution of sucrose, **(C)** log τ (lifetime values were measured in nanoseconds) vs. log η plot in sucrose solutions with increasing viscosity (R^2 = 0.99).

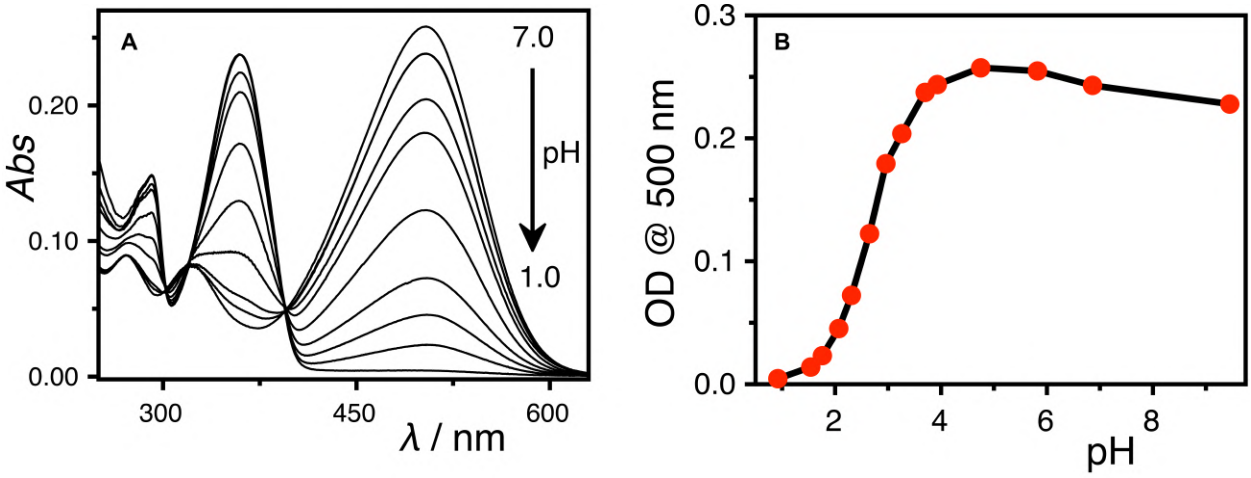

Fig. S3. (A) pH titration of **QR** and **(B)** absorption vs. pH plot.

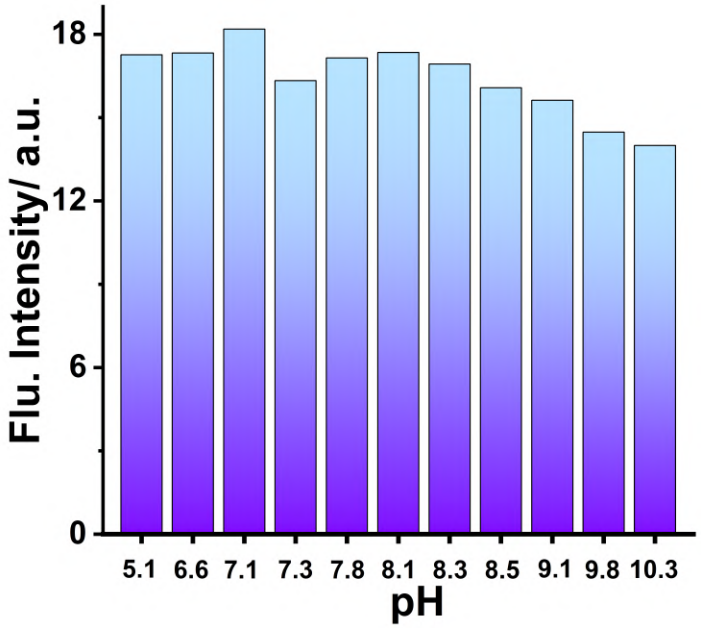

Fig. S4. Bar plot shows the fluorescence intensity of **QR** in the pH range of 5 – 10. Sd $\pm$ 5%

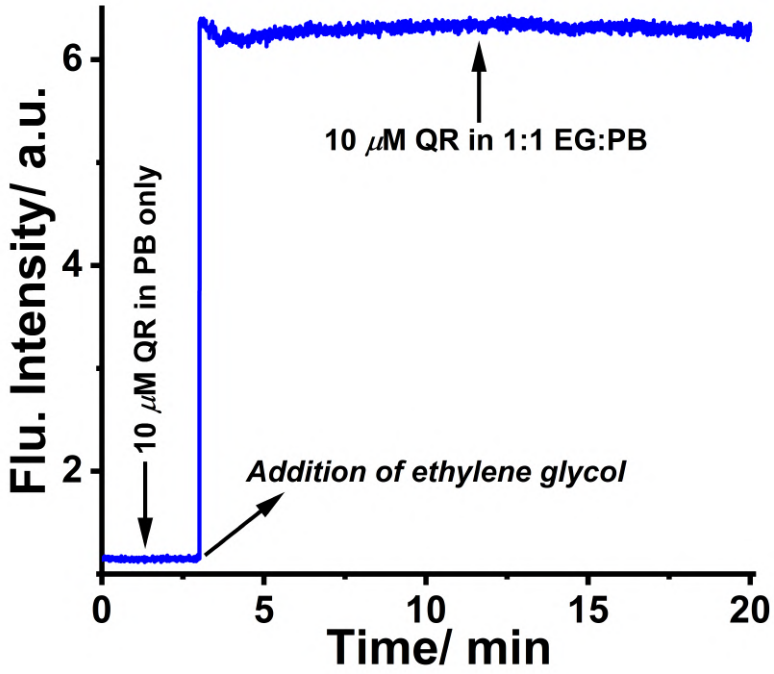

Fig. S5. Fluorescence kinetics of 10 μM **QR** shows the instantaneous emission enhancement with the addition of ethylene glycol (EG) in phosphate buffer (PB).

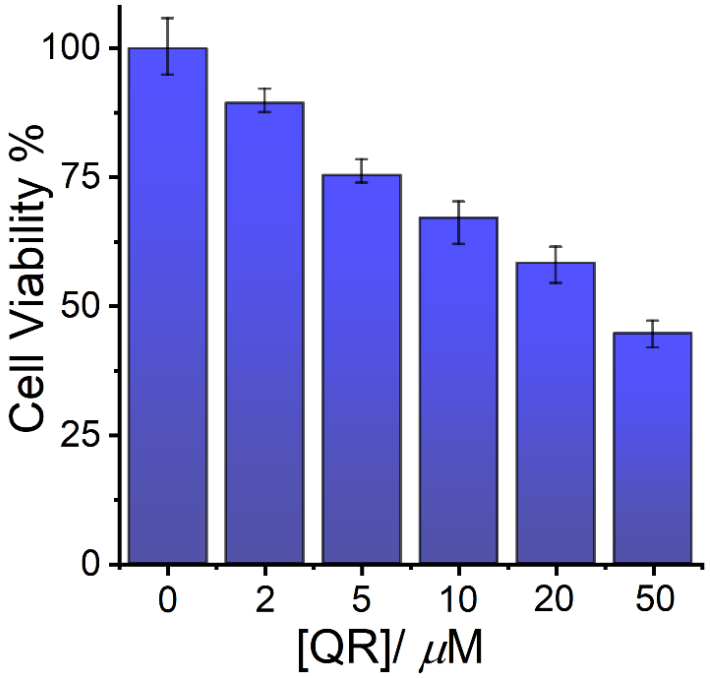

Fig. S6. Cell viability plot with increasing concentrations (0 – 20 μM) of **QR** in U-87 MG cells.

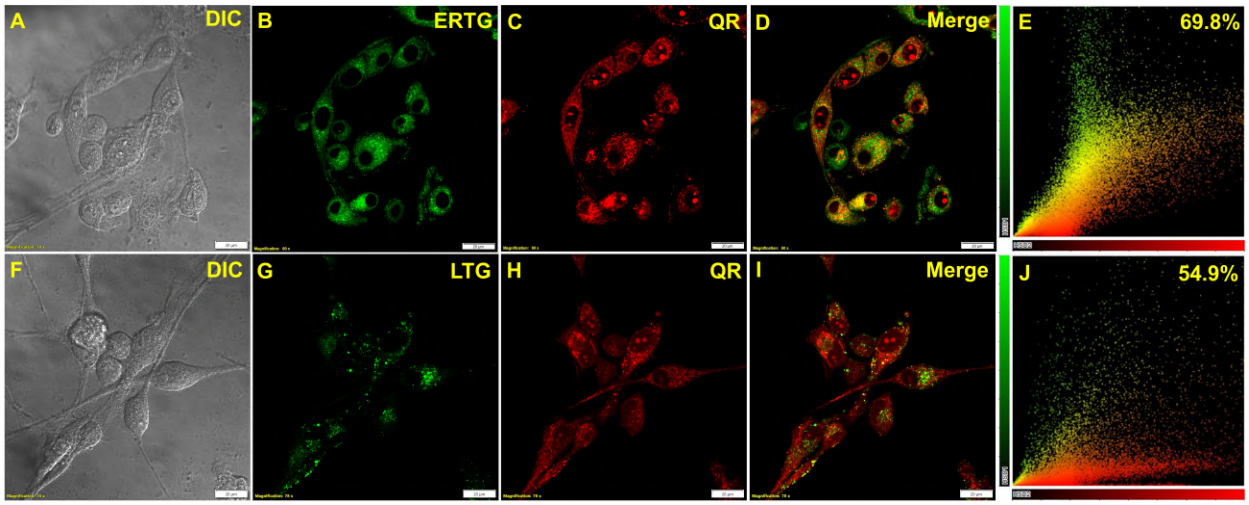

Fig. S7. Confocal live-cell colocalization experiments in U-87 MG cells. **(A)**, and **(F)** show DIC images; **(B)** and **(G)** show the FITC channel images stained with 0.3 μM ER-Tracker Green and LysoTracker Green; **(C)** and **(H)** show the TRITC channel images stained with 5 μM **QR**; **(D)** and **(I)** show the corresponding merge images; **(E)** and **(J)** show the scatter plots that yield respective Pearson's correlation coefficients (scale bar: 20 μm).

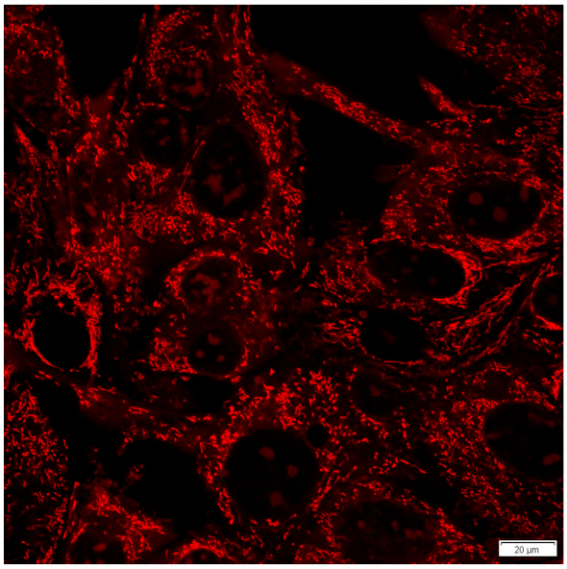

Fig. S8. Confocal live-cell colocalization experiments in CHO cells stained with 5 μM **QR** (scale bar: 20 μm).

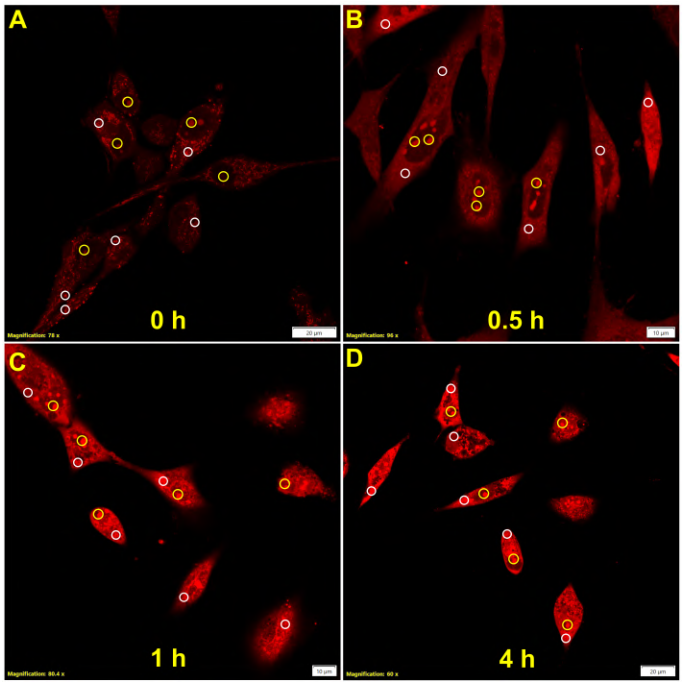

Fig. S9. Confocal microscopy images of U-87 MG cells stained with 5 μM **QR** and treated with monensin; **(A)** incubated with **QR** only, treated with 20 μM monensin for **(B)** 30 min, **(C)** 1 h, and **(D)** 4 h. The circles indicate the regions of interest (ROI) selected for quantifying the change in viscosity in both cases (white circles: mitochondria, yellow circles: nucleolus).

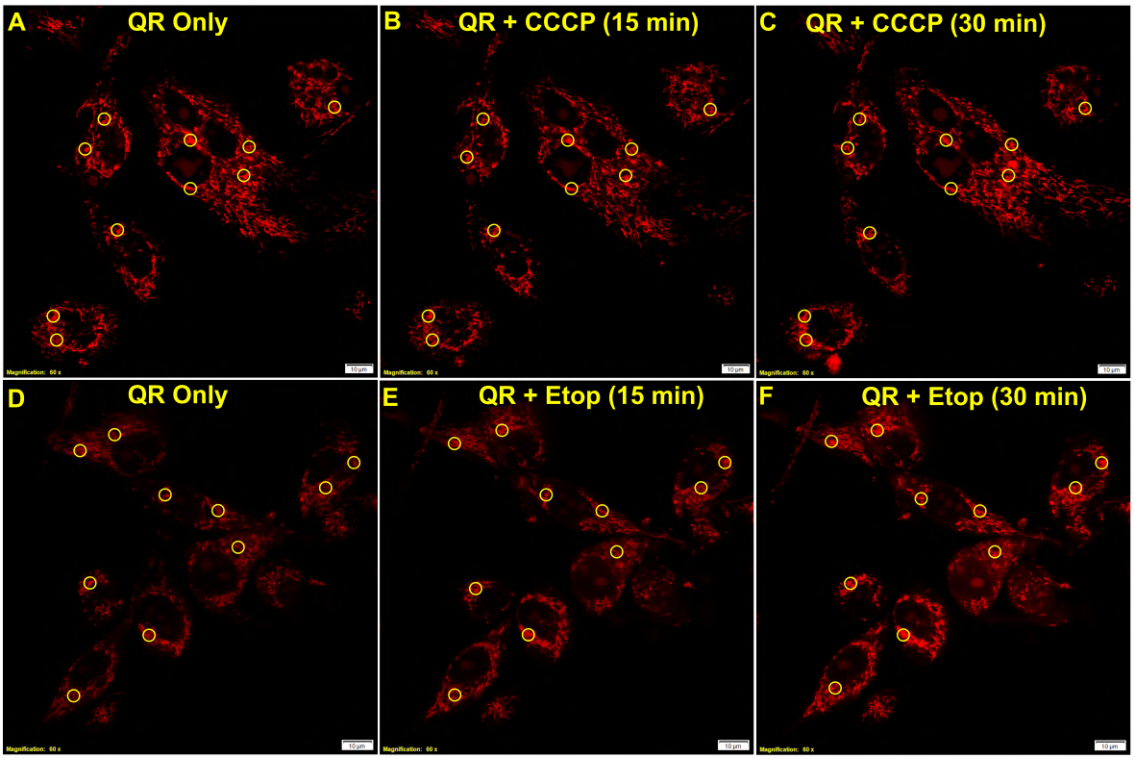

Fig. S10. Confocal microscopy images of U-87 MG cells stained with 5 μM **QR** and treated with CCCP and etoposide; **(A)** & **(E)** incubated with **QR** only, treated with 20 μM CCCP for **(B)** 15 min, **(C)** 30 min, **(D)** bar plot shows no change in the intensity even after membrane potential uncoupling; treated with 50 μM etoposide for **(F)** 15 min. The circles indicate the regions of interest (ROI) selected for quantifying the change in viscosity in both cases.

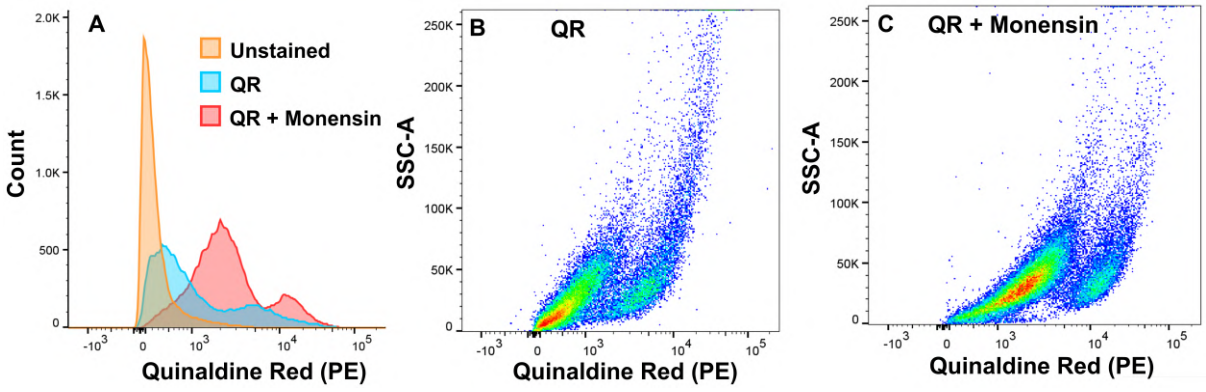

Fig. S11. Flow cytometry analysis of live U-87 MG cells stained with **QR** before and after treatment with monensin. **(A)** shows the representative histogram of unstained cells, only **QR**-stained cells, and monensin-treated **QR**-stained cells, **(B)** and **(C)** show the corresponding distributions of population.

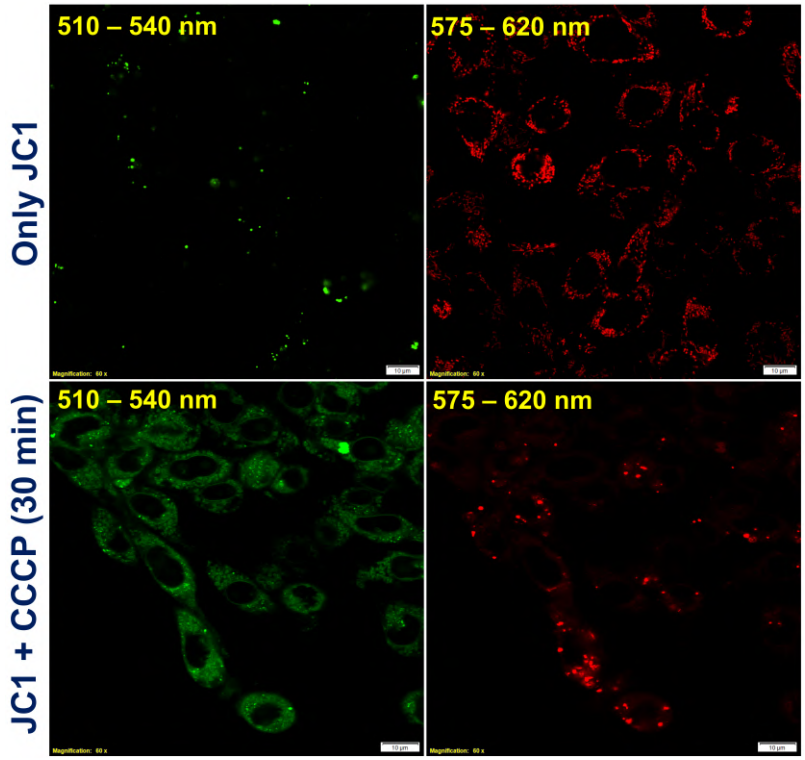

Fig. S12. CLSM images of U-87 MG cells stained with 10 μM JC-1 dye.

Note: For this experiment, live U-87 MG cells were incubated with 10 μM JC-1 dye for 10 minutes at 37 ^{o}C in the dark, washed, and treated with 20 μM CCCP for 30 minutes. Alongside, only JC-1-stained cells were also taken to compare the results. The JC-1 monomer and aggregate species were simultaneously monitored by using a 488 nm excitation laser. The emission channel was set at 510 – 540 nm (monomer emission) and 575 – 620 nm (aggregate emission). CCCP untreated cells showed aggregation emission (orange-red) only whereas treated cells could be visualized only in the monomer emission (green) channel. Hence, it is evident that 20 μM CCCP can disrupt the mitochondrial membrane potential in U-87 MG cells.

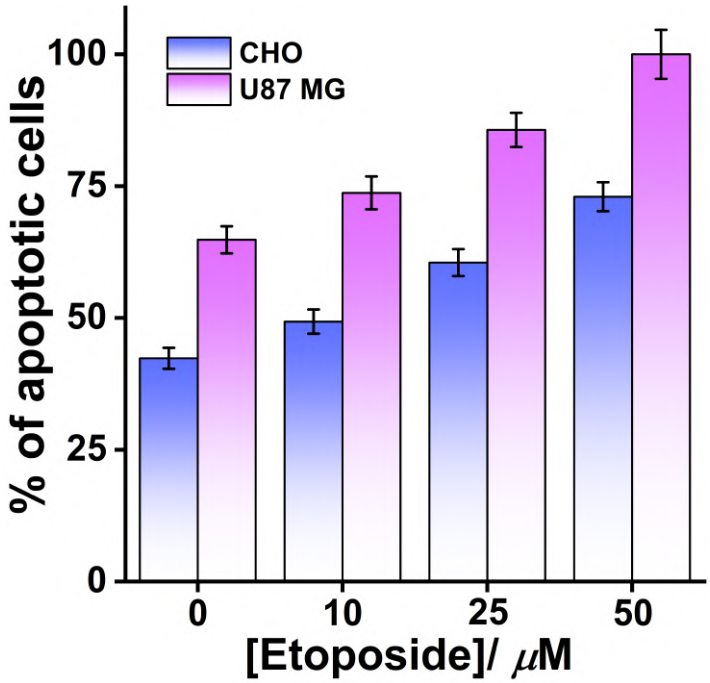

Fig. S13. Determination of cellular ROS by DCFDA (2',7'–dichlorofluorescin diacetate) assay in CHO and U-87 MG cells upon Etoposide treatment in different concentrations (10 – 50 μM).

Note: For this, we have used DCFDA - Cellular ROS Assay Kit which uses the cell-permeant reagent 2',7'–dichlorofluorescin diacetate (DCFDA) to quantitatively assess reactive oxygen species (ROS) in live cells. The DCFDA assay protocol is based on the diffusion of DCFDA into the cell. Thereafter, it is deacetylated by cellular esterases to a non-fluorescent compound, which is later oxidized by ROS into 2',7'–dichlorofluorescein (DCF). DCF is highly fluorescent and is monitored by fluorescence intensity @ 535 nm with excitation at 485 nm. Both normal (CHO) and cancer (U-87 MG) cell lines were taken to compare the ROS levels and it was found from the result that U-87 MG cells had higher ROS levels. The maximum Etoposide concentration was maintained at 50 μM same as used in the mitochondrial viscosity induction experiment.

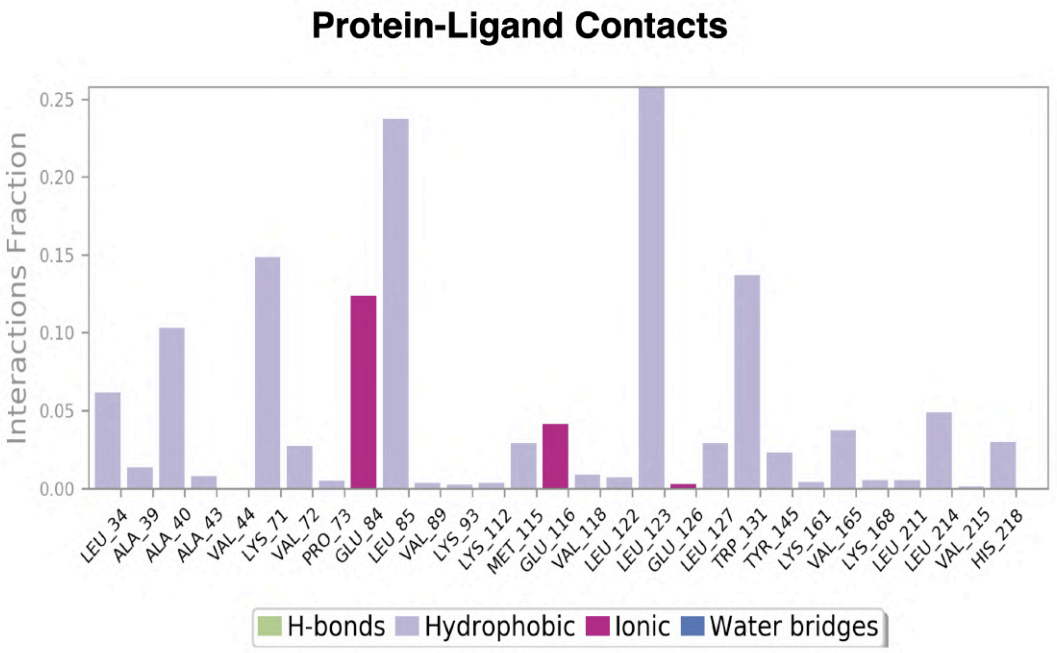

Fig. S14. The interaction of the protein with the ligand monitored throughout the MD simulation for t = 0 – 100 ns.

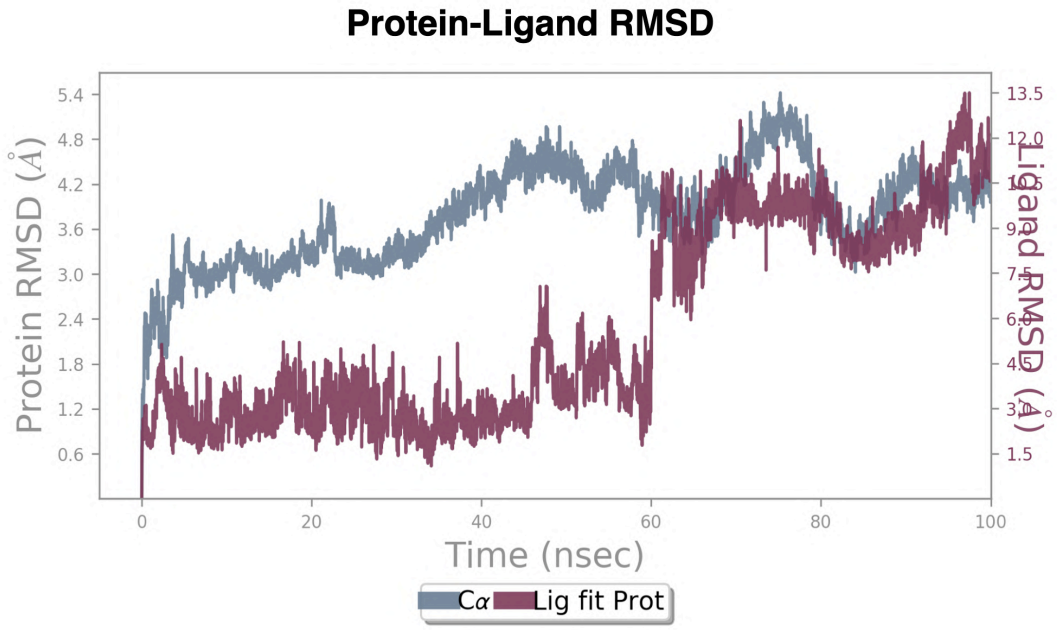

Fig. S15. The root mean square deviation (RMSD) shows the average change in displacement of protein and ligand atoms with respect to a reference frame (here time, t = 0 – 150 ns).

Note: Protein RMSD – The above plot shows the RMSD evolution of a protein (left Y-axis). All protein frames are first aligned on the reference frame backbone, and then the RMSD is calculated based on the atom selection. Monitoring the RMSD of the protein gives insights into its structural conformation throughout the simulation. RMSD analysis can indicate if the simulation has equilibrated — its fluctuations towards the end of the simulation are around some thermal average structure. Changes of the order of 1-3 Å are perfectly acceptable for small, globular proteins.

Ligand RMSD – Ligand RMSD (right Y-axis) indicates how stable the ligand is with respect to the protein and its binding pocket. In the above plot, 'Lig fit Prot' shows the RMSD of a ligand when the protein-ligand complex is first aligned on the protein backbone of the reference and then the RMSD of the ligand heavy atoms is measured. If the values observed are significantly larger than the RMSD of the protein, then it is likely that the ligand has diffused away from its initial binding site.

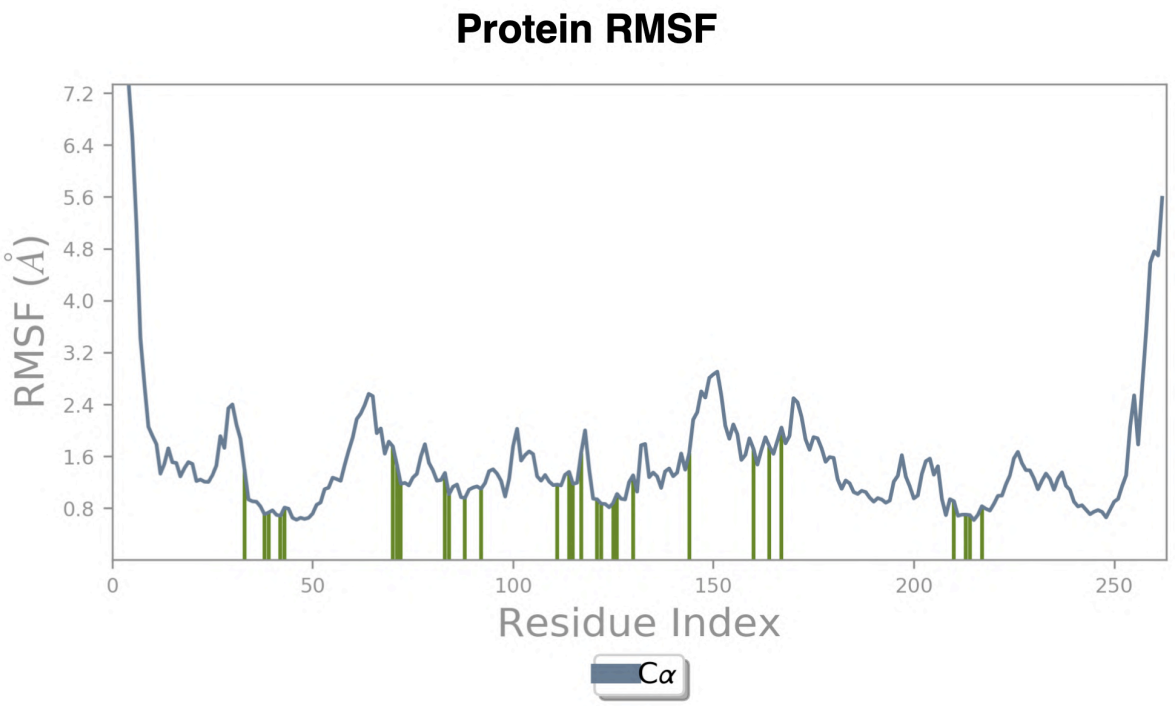

Fig. S16. The root mean square fluctuation (RMSF) for characterizing the local changes along the protein chain.

Note: On this plot, peaks indicate areas of the protein that fluctuate the most during the simulation. Typically, the tails (N- and C-terminal) fluctuate more than any other part of the protein. Secondary structure elements like alpha helices and beta strands are usually more rigid than the unstructured part of the protein, and thus fluctuate less than the loop regions. The protein residues that interact with the ligand are marked with green-colored vertical bars.

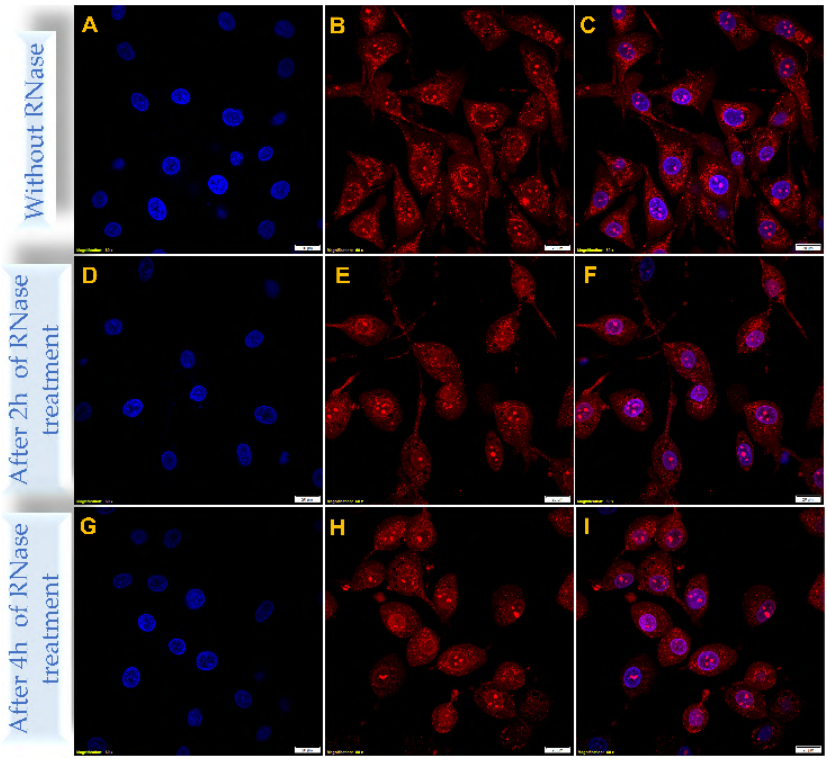

Fig. S17. Confocal microscopy images of U-87 MG cells stained with 8 μM Hoechst 33342 (left panel), 5 μM **QR** (middle panel), and merge images of blue and red channel (right panel); intracellular localization (A-C) before RNase treatment, (D-F) after 100 μM RNase treatment for 2h, and (G-I) 100 μM RNase treatment for 4h. (Scale bar: 20 μm)

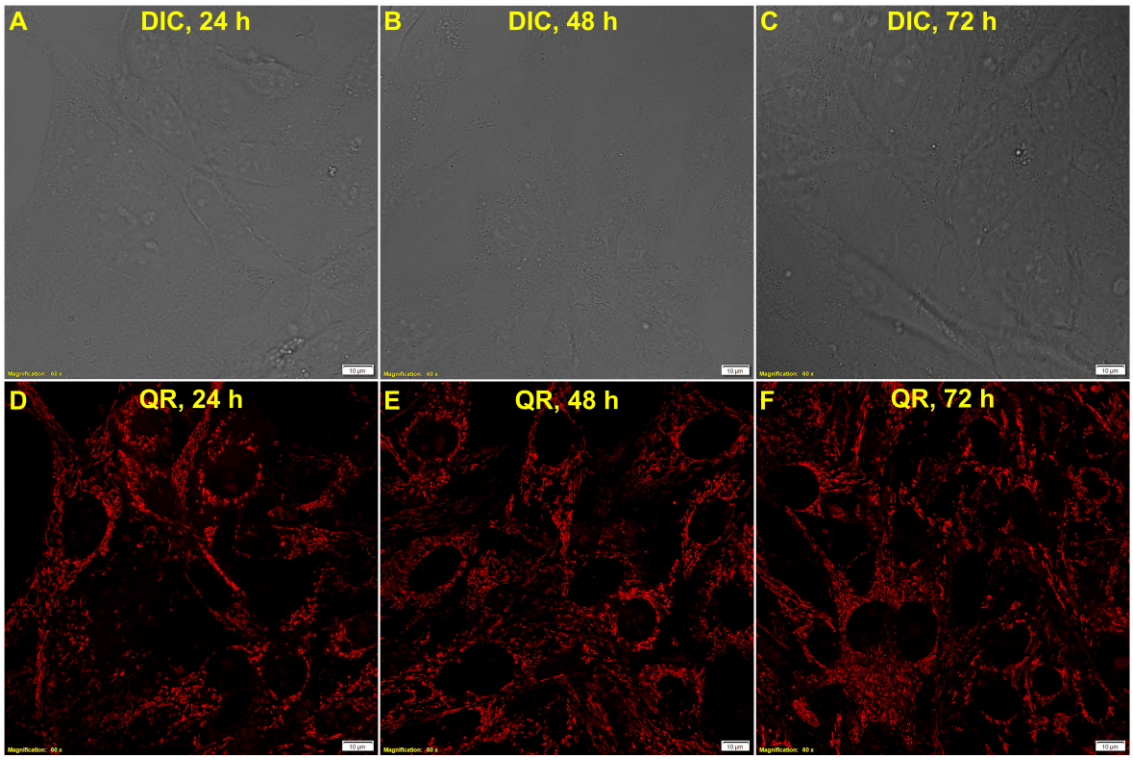

Fig. S18. CLSM images of U-87 MG cells stained with **QR** and imaged after different periods (24 h, 48 h, and 72 h). (A – C) show the DIC images and (D – F) show corresponding TRITC channel images of cells stained with **QR**.

References

1. B. Delley, D. E. Ellis, A. J. Freeman, E. J. Baerends and D. Post, *Phys. Rev. B*, 1983, **27**, 2132-2144.
2. J. P. Perdew, K. Burke and M. Ernzerhof, *Phys. Rev. Lett.*, 1996, **77**, 3865-3868.
3. K. J. Bowers, D. E. Chow, H. Xu, R. O. Dror, M. P. Eastwood, B. A. Gregersen, J. L. Klepeis, I. Kolossvary, M. A. Moraes, F. D. Sacerdoti, J. K. Salmon, Y. Shan and D. E. Shaw, 2006, Page 43.
4. K. Liu, E. Watanabe and H. Kokubo, *J. Comput. Aided Mol. Des.*, 2017, **31**, 201-211.
5. C. D. Schönsee and T. D. Bucheli, *J. Chem. Eng. Data*, 2020, **65**, 1946-1953.
6. M. A. Haidekker and E. A. Theodorakis, *J. Biol. Eng.*, 2010, **4**, 1-14.
7. J. R. Lakowicz, *Principles of Fluorescence Spectroscopy*, Third Ed., 2006, New York, Springer.